Inorganica Chimica Acta, *110* (1985) 7–13

Coordination Chemistry of Lanthanides with Cryptands. An X-ray and Spectroscopic Study of the Complex $Nd_2(NO_3)_6[C_{18}H_{36}O_6N_2]\cdot H_2O$*

F. BENETOLLO

Istituto di Chimica e Tecnologia dei Radioelementi del C.N.R., Corso Stati Uniti, 35141 Padua, Italy

G. BOMBIERI

Istituto di Chimica Farmaceutica e Tossicologica, Università di Milano, Viale Abruzzi 42, 20131 Milan, Italy

A. CASSOL, G. DE PAOLI

Dipartimento di Chimica Inorganica, Metallorganica e Analitica, Università di Padova, Via Marzolo 1, 35131 Padua, Italy

and J. LEGENDZIEWICZ

Institute of Chemistry, University of Wrocław, 50383 Wrocław, Poland

Received October 25, 1984

Abstract

By reacting neodymium nitrate hexahydrate with the cryptand ⟨222⟩ in methanol, the complex $Nd_2(NO_3)_6[C_{18}H_{36}O_6N_2]\cdot H_2O$ was obtained and analyzed by single-crystal X-ray diffraction. The cell is triclinic $P1$ with $a = 14.870(2)$ Å, $b = 13.261(2)$ Å, $c = 8.832(1)$ Å, $\alpha = 91.2(1)^\circ$, $\beta = 93.4(1)^\circ$, $\gamma = 87.6(1)^\circ$, $Z = 2$ and $U = 1736.6$ Å^3. The structure was refined by least-squares methods to the conventional $R = 0.039$ for 6177 observed reflections. The compound contains the cations $[Nd\langle 222\rangle(NO_3)]^{2+}$ and the anions $[Nd(NO_3)_5\cdot H_2O]^{2-}$, and is isostructural with the samarium analogue. Solid state fluorescence spectra of the title complex were measured at room and liquid nitrogen temperature, and the transitions $^4F_{3/2} \rightarrow {}^4I_{9/2}$ and $^4F_{3/2} \rightarrow {}^4I_{11/2}$ analyzed.

Introduction

Three examples of structures of lanthanide complexes with the cryptand ⟨222⟩ are reported in the literature: two nitrato complexes $[La(NO_3)_2\langle 222\rangle]_3[La(NO_3)_6]\cdot 2MeOH$ [1], $Sm(NO_3)\langle 222\rangle][Sm(NO_3)_5\cdot H_2O]$ [2] and the perchlorato complex $[Eu(ClO_4)\langle 222\rangle][ClO_4]_2$ [3]. These compounds show in the solid state the presence of crystallographically distinct ions: $[La(NO_3)\langle 222\rangle]^+$, $[Sm(NO_3)\langle 222\rangle]^{2+}$, $[Eu(ClO_4)_2\langle 222\rangle]^+$ and $[La(NO_3)_6]^{3-}$, $[Sm(NO_3)_5\cdot H_2O]^{2-}$ and ClO_4^- respectively. In the cations the lanthanide ions are enclosed in a ⟨222⟩ molecule forming a cryptate with one or two oxyanions residing between two strands of the oxygen atoms, and taking part of the coordination sphere of the lanthanide ions. The resulting coordination number is 10 for samarium and europium cryptates and 12 for the lanthanum one. The crystal structure determination of the title compound was undertaken in order to verify the eventual variation of the coordination mode along the lanthanoid series. Furthermore, the fluorescence and absorption spectra of the crystals of the neodymium cryptate were measured and the results are discussed.

Experimental

Preparation of the Compound

The complex was prepared by mixing methanolic solutions of neodymium nitrate hexahydrate and ⟨222⟩ in the molar ratio 1/1. The crude product was crystallized from methanol and analyzed. *Anal.* Calcd. for $C_{18}H_{38}N_8O_{25}Nd_2$: C, 20.49; H, 3.63; N, 10.62. Found: C, 20.37; H, 3.54; N, 10.54%.

X-ray Measurements and Structure Determination

The crystal and refinement data are summarized in Table I. The X-ray intensity data were collected on a four-circle Philips PW 1100 automated diffractometer with graphite monochromated MoKα radiation. The unit cell was determined on the basis of 25 strong reflections, found by mounting the crystal at random and varying the orientation angles Φ and χ in the range of 120° each with the detector position varying between $\theta = 6^\circ$ and $\theta = 10^\circ$. For the

---

*$C_{18}H_{36}O_6N_2$ = ⟨222⟩ = 4,7,13,16,21,24-hexaoxa-1,10-diaza-bicyclo[8.8.8]-hexacosane.

0020-1693/85/$3.30

© Elsevier Sequoia/Printed in Switzerland

TABLE I. Crystal Data.

Compound	$[Nd\langle 222\rangle(NO_3)]^{2+}$ $[Nd(NO_3)_5\cdot H_2O]^{2-}$
Formula	$C_{18}H_{36}O_6N_2Nd_2(NO_3)_6\cdot H_2O$
M	1055
Space group	$P\bar{1}$
Crystal system	triclinic
a (Å)	14.870(2)
b (Å)	13.261(2)
c (Å)	8.832(1)
α (°)	91.2(1)
β (°)	93.4(1)
γ (°)	87.6(1)
U (Å^3)	1736.6
Z	2
Dc (g cm^{-3})	2.02
$F(000)$	1044
Radiation (λ/Å)	MoKα (0.7107)
Reflections measured	6177
Scan method	$\theta/2\theta$
Scan speed (min^{-1})	1.8
Scan width (°)	1.2
Background count(s) counting time	10
$2\theta_{max}$ (°)	50
σ limit $|I > n\sigma(I)|$	n = 3
Unique observed reflections	3678
R ($R = \Sigma|F_o| - |F_c|/\Sigma|F_o|$)	0.039
μ(Mo-Kα) (cm^{-1})	28.8

TABLE II. Atomic Coordinates and Standard Deviations ($\times 10^4$) in Parentheses.

Atom	x	y	z
Nd(1)	2032.7(4)	3095.4(4)	1302.4(6)
Nd(2)	3154.2(4)	8156.2(4)	5514.6(6)
O(1)	3099(6)	1586(7)	822(10)
O(2)	1349(7)	1446(7)	173(11)
O(3)	3124(5)	3400(6)	3469(7)
O(4)	1871(5)	2152(7)	3687(9)
O(5)	2402(6)	4940(6)	857(10)
O(6)	1117(7)	4482(9)	2566(11)
O(7)	3561(5)	6829(6)	3502(9)
O(8)	4668(5)	7318(6)	4961(8)
O(9)	4913(6)	6192(7)	3217(10)
O(10)	4581(5)	9291(6)	6113(9)
O(11)	3281(5)	9972(6)	6514(9)
O(12)	4481(7)	10762(7)	7178(11)
O(13)	3822(6)	8175(7)	8320(10)
O(14)	2389(6)	8203(6)	8043(9)
O(15)	3036(8)	8157(8)	10279(10)
O(16)	3294(6)	6374(6)	6671(10)
O(17)	2011(5)	6748(6)	5542(9)
O(18)	2218(7)	5312(7)	6590(11)
O(19)	1946(6)	8186(8)	3236(10)
O(20)	1637(6)	9064(7)	5220(11)
O(21)	651(7)	8967(10)	3328(14)
O(22)	2116(5)	3009(6)	−1543(8)
O(23)	917(5)	3753(6)	−740(9)
O(24)	994(6)	3375(8)	−3128(9)
Ow	3641(5)	9056(6)	3208(8)
N(1)	3771(6)	3538(9)	643(11)
N(2)	299(7)	2620(12)	2015(13)
N(3)	4397(6)	6754(7)	3867(10)
N(4)	4128(7)	10022(8)	6612(10)
N(5)	3081(8)	8183(7)	8926(11)
N(6)	2494(7)	6127(8)	6278(10)
N(7)	1395(7)	8756(9)	3934(14)
N(8)	1338(6)	3397(7)	−1843(11)
C(1)	4198(9)	2630(13)	−78(16)
C(2)	4067(9)	1729(12)	831(18)
C(3)	2830(16)	757(15)	−64(34)
C(4)	1947(17)	588(12)	−245(25)
C(5)	444(14)	1189(16)	156(23)
C(6)	−127(10)	2086(20)	627(19)
C(7)	4349(8)	3831(11)	2056(14)
C(8)	3779(8)	4168(9)	3353(13)
C(9)	3029(8)	3032(9)	4977(11)
C(10)	2629(10)	2010(11)	4748(15)
C(11)	1140(10)	1467(12)	3832(17)
C(12)	280(11)	1997(18)	3404(20)
C(13)	3672(10)	4362(13)	−474(15)
C(14)	3209(13)	5260(12)	166(17)
C(15)	1894(13)	5774(13)	1367(26)
C(16)	1339(16)	5491(16)	2432(38)
C(17)	304(18)	4252(20)	3300(22)
C(18)	−213(12)	3611(21)	2269(26)

determination of precise lattice parameters 20 strong reflections with 9° $\leqslant \theta \leqslant$ 14° were considered. The intensities of two standard reflections 3 0 2 and 2 1 1 at 100 reflection intervals showed no greater fluctuations than those expected from Poisson statistics.

The intensity data were collected for Lorentz-polarization effects and for absorption following the method of North *et al.* [4]. The structure was solved using the three-dimensional Patterson and Fourier techniques and refined with blocked matrix (two blocks) least squares with anisotropic thermal parameters assigned to all the non-hydrogen atoms. In all the refinement $w = 1$ was used as it showed reasonable consistency in a test of $w\Delta^2$ for data selectioned with respect both to $|F_o|$ and to λ^{-1} $\sin\theta$. Hydrogen atoms were neither found nor included in calculations.

The anomalous dispersion terms for Nd were taken into account in the refinement [5]. Atomic scattering factors for non-hydrogen atoms were from ref. [5]. Data processing and computation were carried out using the SHELX 76 program package [6]. Final positional parameters are reported in Table II. Interatomic distances and torsion angles are given in Tables III and IV respectively. Observed and calculated structure factors (×10) and thermal parameters are available as Supplementary material (TABLE A).

TABLE III. Interatomic Distances and Standard Deviations (Å) in Parentheses.

(a) Cation			
Nd(1)–N(1)	2.772(9)	C(1)–C(2)	1.48(2)
Nd(1)–N(2)	2.791(11)	C(2)–O(1)	1.46(2)
Nd(1)–O(1)	2.544(9)	O(1)–C(3)	1.39(2)
Nd(1)–O(2)	2.601(10)	C(3)–C(4)	1.34(3)
Nd(1)–O(3)	2.471(7)	C(4)–O(2)	1.47(2)
Nd(1)–O(4)	2.502(8)	O(2)–C(5)	1.40(2)
Nd(1)–O(5)	2.574(8)	C(5)–C(6)	1.50(3)
Nd(1)–O(6)	2.523(11)		
Nd(1)–O(22)	2.523(7)	C(7)–C(8)	1.51(2)
Nd(1)–O(23)	2.521(8)	C(8)–O(3)	1.45(1)
		O(3)–C(9)	1.44(1)
N(1)–C(1)	1.49(2)	C(9)–C(10)	1.51(2)
N(1)–C(7)	1.52(2)	C(10–O(4)	1.43(2)
N(1)–C(13)	1.48(2)	O(4)–C(11)	1.46(2)
		C(11)–C(12)	1.47(2)
N(2)–C(6)	1.52(2)		
N(2)–C(12)	1.50(2)	C(13)–C(14)	1.47(2)
N(2)–C(18)	1.51(3)	C(14)–O(5)	1.46(2)
		O(5)–C(15)	1.39(2)
N(8)–O(22)	1.26(1)	C(15)–C(16)	1.36(4)
N(8)–O(23)	1.26(1)	C(16)–O(6)	1.40(2)
N(8)–O(24)	1.22(1)	O(6)–C(17)	1.45(3)
		C(17)–C(18)	1.44(3)
		O_w···O(7)	2.98(1)
		O_w···O(10)	2.86(1)
		O_w···O(19)	2.82(1)
N–C_{ave}	1.42		
O–C_{ave}	1.43		
C–C_{ave}	1.45		
(b) Anion			
Nd(2)–O(7)	2.555(8)	N(4)–O(10)	1.24(1)
Nd(2)–O(8)	2.538(8)	N(4)–O(11)	1.26(1)
Nd(2)–O(10)	2.674(8)	N(4)–O(12)	1.22(1)
Nd(2)–O(11)	2.557(8)		
Nd(2)–O(13)	2.613(9)		
Nd(2)–O(14)	2.564(8)	N(5)–O(13)	1.25(1)
Nd(2)–O(16)	2.590(8)	N(5)–O(14)	1.25(1)
Nd(2)–O(17)	2.579(8)	N(5)–O(15)	1.20(1)
Nd(2)–O(19)	2.616(9)		
Nd(2)–O(20)	2.514(9)	N(6)–O(16)	1.27(1)
Nd(2)–O_w	2.541(8)	N(6)–O(17)	1.24(1)
		N(6)–O(18)	1.22(2)
N(3)–O(7)	1.26(1)		
N(3)–O(8)	1.26(1)	N(7)–O(19)	1.27(1)
N(3)–O(9)	1.21(1)	N(7)–O(20)	1.24(2)
		N(7)–O(21)	1.22(1)

TABLE IV. Torsion Angles (°) of the (222) Ligand.

N(1)–C(1)–C(2)–O(1)	62.8
C(1)–C(2)–O(1)–C(3)	108.0
C(2)–O(1)–C(3)–C(4)	–175.5
O(1)–C(3)–C(4)–O(2)	15.7
C(3)–C(4)–O(2)–C(5)	–172.0
C(4)–O(2)–C(5)–C(6)	178.6
O(2)–C(5)–C(6)–N(2)	–45.2
N(1)–C(7)–C(8)–O(3)	49.1
C(7)–C(8)–O(3)–C(9)	131.6
C(8)–O(3)–C(9)–C(10)	–158.0
O(3)–C(9)–C(10)–O(4)	–49.6
C(9)–C(10)–O(4)–C(11)	–150.9
C(10)–O(4)–C(11)–C(12)	147.4
O(4)–C(11)–C(12)–N(2)	43.2
N(1)–C(13)–C(14)–O(5)	–48.5
C(13)–C(14)–O(5)–C(15)	–174.8
C(14)–O(5)–C(15)–C(16)	–159.2
O(5)–C(15)–C(16)–O(6)	–19.5
C(15)–C(16)–O(6)–C(17)	–158.1
C(16)–O(6)–C(17)–C(18)	126.8
O(6)–C(17)–C(18)–N(2)	64.0

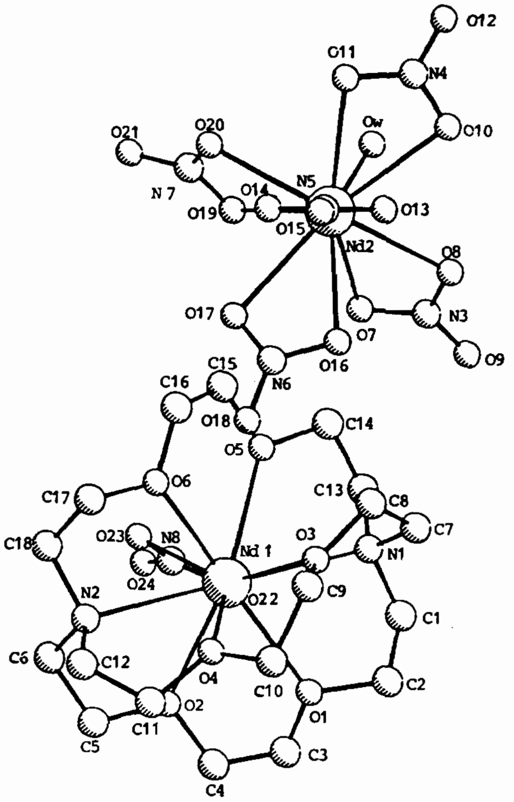

Fig. 1. A perspective view of the molecular structure of $Nd_2(NO_3)_6[C_{18}H_{36}O_6N_2]\cdot H_2O$.

Spectroscopic Measurements

Fluorescence spectra were measured on a spectrophotometer constructed in the Institute for Low Temperature and Structure Research, Polish Academy of Sciences, using a GDM 1000 mono-

TABLE V. Complexes of Lanthanides with ⟨222⟩: A Comparison of the Distances in the Complex Cations (distances are in Å).

Complex	Ionic radii[a]	C.N.	$Ln-N_{(cryptand)}$	$Ln-O_{(cryptand)}$	$Ln-O_{(oxyanion)}$
$[La(NO_3)_2\langle 222\rangle]_3[La(NO_3)_6]\cdot 2MeOH$	1.061	12	2.813–2.848	2.644–2.736	2.626–2.688
$[Nd(NO_3)\langle 222\rangle][Nd(NO_3)_5(H_2O)]$	0.995	10	2.772(9)–2.791(11)	2.471(7)–2.601(10)	2.523(7)–2.521(8)
$[Sm(NO_3)\langle 222\rangle][Sm(NO_3)_5(H_2O)]$	0.964	10	2.748(5)–2.779(6)	2.441(4)–2.566(5)	2.484(4)–2.502(4)
$[Eu(ClO_4)\langle 222\rangle][ClO_4]_2\cdot MeCN$	0.950	10	2.64(3)–2.70(5)	2.44(4)–2.52(3)	2.67(4)–2.71(4)

[a] Ionic radii are taken from ref. 19.

chromator (Carl Zeiss, Jena) and a phase-sensitive detection system equipped with a photomultiplier with S-1 response. An argon laser (ILA 120, Carl Zeiss, Jena) was used as an excitation source. The excitations were performed at 488 nm and 514 nm. Absorption spectra of crystals were measured on a Cary 14 spectrophotometer, at room temperature. Measurements were limited only to the range 9000–5500 Å and only for some electron transitions, because of the crystal size (1 × 1 mm slide), the poor transparency, and because of the own transitions of a ligand.

Results and Discussion

Description of the Structure

The compound is isostructural with the samarium derivative and it is composed of cations $[Nd\langle 222\rangle(NO_3)]^{2+}$ and anions $[Nd(NO_3)_5H_2O]^{2-}$. Figure 1 shows a perspective view of the molecular structure. In the complex cation the neodymium ion is enclosed in the bicyclic ligand, the nitrato group completes the metal coordination and resides, as in the samarium derivative, between two strands of the ⟨222⟩ ligand. In Table V some significant parametes in different lanthanide complexes (La, Nd, Sm and Eu) with the ⟨222⟩ ligand are compared. The trend of the metal ionic radii is respected in the corresponding variation of the bond lengths to the central metal. Apart from the lanthanum derivative which, due to its highest ionic radius can accommodate 12 donor atoms in the coordination sphere, the other three complexes are 10 coordinate with a distorted square-capped antiprismatic geometry, two nitrogen atoms capping the two 'square' faces. The mean values of the bond length and angles in ⟨222⟩ molecule compare with the values of literature with C–C = 1.45 Å O–C = 1.43 Å, N–C = 1.50 Å, O–C–C = 110.3°, N–C–C = 111.4°, C–O–C = 114.7° and C–N–C = 110.8°. In addition to the noticeable distortion of the conformation of the coordinate ligand as observed in the samarium derivative, the higher atomic radius of neodymium with respect to samarium favours a further distortion in the macrocyclic ligand being the Nd–O and Nd–N distances higher in comparison to that of samarium, as expected. In the complex anion $[Nd(NO_3)_5H_2O]^{2-}$ the NO_3 groups are all bidentate, and as in the samarium derivative, the Nd–O bond lengths range from 2.514(9) to 2.674(8) Å with a mean value of 2.58(4) Å, comparable with that found in the hexanitrato anion $[Nd(NO_3)_6]^{3-}$ of 2.59(4) Å [7]. However, different from $[Nd(NO_3)_6]^{3-}$ which is of D_{2h} symmetry, the Nd–O bond distances are not symmetrical. In particular two nitrato groups, O(10) and O(11); O(19) and O(20) which comprise between them the water molecule, show a difference of about 0.1 Å in the $Nd-O_{(nitrate)}$ bond for both nitrates, probably related to the presence of coordinate water. This H_2O molecule, as in the samarium derivative, makes weak hydrogen bonds to different anions with O(12)′ (at 1 – x, 2 – y, 1 – z) and O(15)″ (at x, y, 1 – z) with values 2.84 Å and 2.93 Å respectively, while the O(12)′–O(w)–O(15)″ angle is 101.4° (the corresponding values in the samarium derivative are 2.87 Å, 2.95 Å and 100.5°). The difference in the ionic radii does not play a significant role in the molecular packing, being the intermolecular contacts of the same order in the two isomorphous and isostructural compounds. This difference affects the conformation of the macrocyclic ligand because of its high flexibility.

Fluorescence and Absorption Spectra

Fluorescence of the neodymium cryptate crystal was measured at room and liquid nitrogen temperatures. However, at room temperature the crystals suffered decomposition under excitation. The Nd^{3+} fluorescence originates totally from $^4F_{3/2}$ level that is split into two Stark components in non-cubic systems. The fluorescence spectra corresponding to the $^4F_{3/2} \rightarrow {}^4I_{9/2}$, $^4I_{11/2}$ transitions are shown in Fig. 2 (a and b). In the luminescence spectra the lines were found between 10970–11630 cm^{-1}, corresponding to transitions which originate in the $^4F_{3/2}$ manifold and terminate on levels of the $^4I_{9/2}$ manifold, the lines recorded between 9200–9700 cm^{-1} being attributed to the $^4F_{3/2} \rightarrow {}^4I_{11/2}$ transition. We found that the spectra are dependent on the excitation wavelength. In

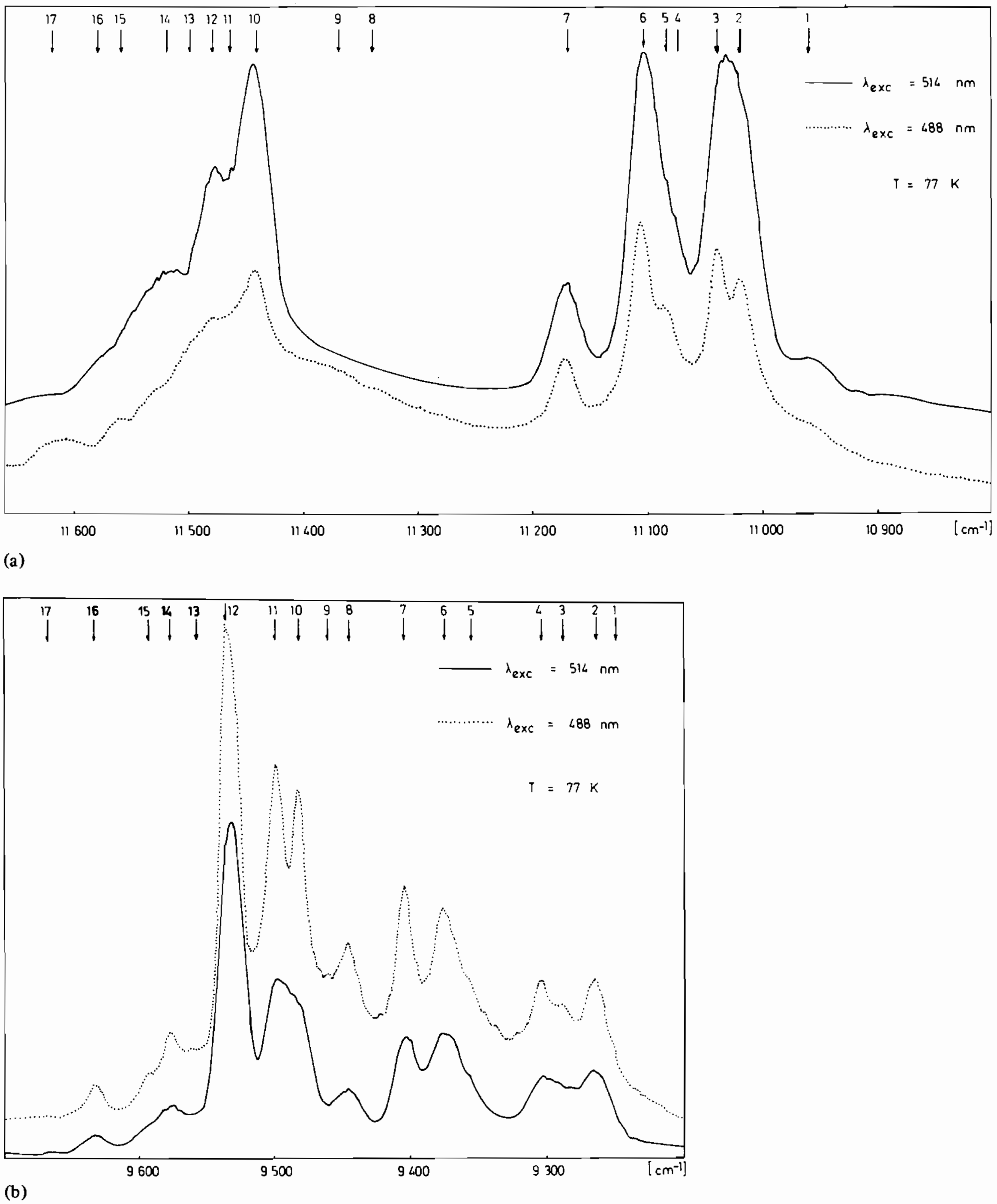

Fig. 2. Fluorescence spectra of the neodymium cryptate, at liquid nitrogen temperature: (a) for $^4F_{3/2} \rightarrow {}^4I_{9/2}$ transition. (b) for $^4F_{3/2} \rightarrow {}^4I_{11/2}$ transition.

Table VI the peak positions of fluorescence spectra for 488 and 514 nm excitation wavelengths are listed. For non-cubic systems the $^4F_{3/2} \rightarrow {}^4I_{9/2}$ and $^4F_{3/2} \rightarrow {}^4I_{11/2}$ transitions should be split at elevated temperature into 10 and 12 Stark components, respectively. We have found 17 Stark components for both of these transitions, in the spectra recorded at 77 K (Table VI).

For non-centrosymmetric lanthanide crystals (except the hypersensitive transitions [8]) no strong-

TABLE VI. The Peak Position (cm^{-1}) for $^4F_{3/2} \rightarrow {}^4I_{9/2}$ and $^4F_{3/2} \rightarrow {}^4I_{11/2}$ Transitions in Fluorescence Spectra of $C_{18}H_{36}O_6N_2$-$Nd_2(NO_3)_6 \cdot H_2O$ Crystal at 77 K, and the Corresponding Stark Components for I Site of Nd^{3+} Ion in Crystal.

No.	$^4F_{3/2} \rightarrow {}^4I_{11/2}$				$^4F_{3/2} \rightarrow {}^4I_{9/2}$			
	Peak position (cm^{-1})		I site of Nd^{3+} ion		Peak position (cm^{-1})		I site of Nd^{3+} ion	
	λ_{exc} = 488 nm	λ_{exc} = 514 nm			λ_{exc} = 488 nm	λ_{exc} = 514 nm		
1	9248	9240			10970	10960		10970
2	9260	9260		9260	11020	11020		11020
3	9286	9286			11038	11040	11038	
4	9300	9300		9300		11075		
5	9345	9356	9345		11085	11082	11085	
6	9375	9375	9375		11105	11104		11105
7	9400	9405		9400	11170	11170	11170	
8	9450	9450		9450	11330			
9	9460				11370			
10	9480	9480	9480		11440	11440		11440
11	9500	9497		9500	11463	11460		
12	9530	9532	9530		11485	11485		11485
13	9560	9532		9560	11498	11500		
14	9580	9578	9580		11510	11520	11510	
15	9592	9592			11560	11550	11560	
16	9635	9634	9635			11580		
17	9665	9665			11610	11630		

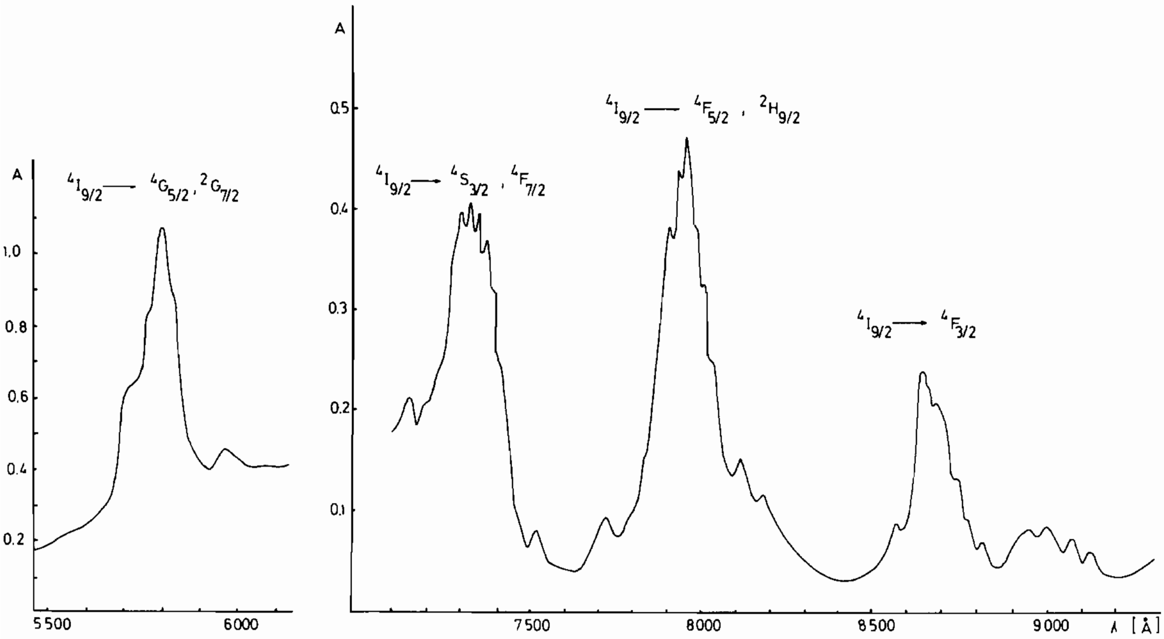

Fig. 3. The absorption spectrum measured at 239 K.

vibronic components were observed in the fluorescence spectra. Then, no vibronic transitions are expected for the measured crystals spectra. The observed composite structure of electronic transitions can be explained by assuming that in the crystal investigated the Nd^{3+} ions occupy two different symmetric positions. Such a behaviour was observed for lanthanide ions in many crystals [9–16]. For Nd^{3+} ions, Stark components for different sites were determined and energy diagrams were proposed [9–

12] in crystals of CaF_2-doped Nd^{3+}, $Nd_{1-x}Y_xP_5O_{14}$, $CaLa_4(SiO_4)_3O$–Nd, CaF_2 doped with Nd_2O_3 or NdOF [9–12].

As reported in Table VI, two double sequences of 5 and 6 Stark components were found for the transitions $^4F_{3/2} \rightarrow {}^4I_{9/2}$ and $^4F_{3/2} \rightarrow {}^4I_{11/2}$ respectively and in each case they resulted mutually displaced of about 75 cm^{-1}. These levels could be assigned to one Nd^{3+} ion site, the remaining Stark components corresponding to the second Nd^{3+} ion site. The $^4F_{3/2}$ level splitting of about 75 cm^{-1} seems to correspond to that found in the absorption spectrum ($^4I_{9/2} \rightarrow {}^4F_{3/2}$)*. The absorption bands observed are due to transitions from $^4I_{9/2}$ ground state multiplet to $^4F_{3/2}$, $^2H_{9/2}$, $^4F_{5/2}$, $^4F_{7/2}$, $^4S_{3/2}$, $^4G_{5/2}$, $^2G_{7/2}$ levels and higher excited levels. The hypersensitive transition $^4I_{9/2} \rightarrow {}^5G_{5/2}$ of Nd^{3+} ion is shown in Fig. 3. The relative intensity in this band is not far from the transitions observed for neodymium compounds with aminoacids [17, 18].

References

1 F. A. Hart, M. B. Hursthouse, M. K. Abdul Malik and S. Moorhouse, *J. Chem. Soc., Chem. Commun.*, 549 (1978).

2 J. H. Burns, *Inorg. Chem., 18,* 3044 (1979).

3 M. Ciampolini, P. Dapporto and N. Nardi, *J. Chem. Soc., Dalton Trans.*, 974 (1979).

4 A. C. T. North, D. C. Phillips and F. Mathews, *Acta Crystallogr., Sect. A:, 24,* 351 (1968).

5 'International Tables for X-ray Crystallography, Vol. 4, 2nd. edn.', Kynoch Press, Birmingham, 1974, p. 101.

6 G. M. Sheldrick, 'SHELX 76', University of Cambridge, 1976.

7 J.-C. G. Bünzli, B. Klein, D. Wessner, K. I. Schenk, G. Chapuis, G. Bombieri and G. De Paoli, *Inorg. Chim. Acta, 54,* L43 (1981).

8 B. R. Judd, *Phys. Scr., 21,* 543 (1980).

9 Yu. K. Voronko, A. A. Kaminskii and V. V. Osiko, *Zh. Eksp. Teor. Fiz., 49,* 420 (1965); engl. transl., *Sov. Phys. JETP, 22,* 295 (1966).

10 W. W. Krühler, G. Huber and H. G. Danielmeyer, *V. Nekvasil Appl. Phys., 8,* 261 (1975).

11 J. C. Toledano, *J. Chem. Phys., 57,* 1046 (1972).

12 A. O. Ivanov, L. G. Morozova, I. V. Mochalov and V. A. Fodorov, *Opt. Spectrosk., 42,* 556 (1977); engl. transl., *Opt. Spectrosc. (USSR), 42,* 311 (1977).

13 M. Asano and J. A. Konigstein, *Chem. Phys., 42,* 369 (1979).

14 L. V. Haley, B. Jacquier and J. A. Konigstein, *Can. J. Chem., 59,* 441 (1981).

15 A. A. Kaminskii, 'Laser Crystals, Their Physics and Properties', Springer-Verlag, Berlin/Heidelberg/New York, 1981 and refs. therein.

16 M. D. Kurz and J. C. Wright, *J. Lumin., 15,* 169 (1977).

17 J. Legendziewicz, E. Huskowska, A. Waskowska and Gy. Argay, *Inorg. Chim. Acta, 92,* 151 (1984).

18 J. Legendziewicz, E. Huskowska, Gy. Argay and A. Waskowska, *Inorg. Chim. Acta, 95,* 57 (1984).

19 R. D. Shannon, *Acta Crystallogr., Sect. A:, 32,* 751 (1976).

---

*A more precise energy assignment could be possible by measuring the spectra in the range of the Kramer's doublet ($^4I_{9/2} \rightarrow {}^2P_{1/2}$).